Ultrashort pulse laser lift-off processing of InGaN/GaN light-emitting diode chips

Nursidik Yulianto[1,2,3,*], Grandprix T. M. Kadja[4,5], Steffen Bornemann[1,2], Soniya Gahlawat[6,7], Nurhalis Majid[3,8], Kuwat Triyana[9], Fatwa F. Abdi[6], Hutomo Suryo Wasisto[1,2,*], Andreas Waag[1,2]

[1] Institute of Semiconductor Technology (IHT), Technische Universität Braunschweig, Hans-Sommer-Straße 66, Braunschweig 38106, Germany

[2] Laboratory for Emerging Nanometrology (LENA), Technische Universität Braunschweig, Langer Kamp 6, Braunschweig 38106, Germany

[3] Research Centre for Physics, Indonesian Institute of Sciences (LIPI), Jl. Kawasan Puspiptek No. 441-442, 15314 Tangerang Selatan, Indonesia

[4] Division of Inorganic and Physical Chemistry, Faculty of Mathematics and Natural Sciences, Institut Teknologi Bandung, Jl Ganesha 10, Bandung 40132, Indonesia

[5] Research Center for Nanosciences and Nanotechnology, Institut Teknologi Bandung, Jl. Ganesha 10, Bandung 40132, Indonesia

[6] Institute for Solar Fuels, Helmholtz-Zentrum Berlin für Materialien und Energie GmbH, Institute for Solar Fuels, Hahn-Meitner-Platz 1, Berlin 14109, Germany

[7] Department of Chemistry, Indian Institute of Technology Delhi, New Delhi 110016, India

[8] Institute of Energy Research and Physical Technologies, Technische Universität Clausthal, Leibnizstraße 4, Clausthal-Zellerfeld 38678, Germany

[9] Department of Physics, Faculty of Mathematics and Natural Sciences, Universitas Gadjah Mada, Sekip Utara PO Box BLS 21, Yogyakarta 55281, Indonesia

* Corresponding authors.

E-mails: n.yulianto@tu-braunschweig.de (N.Y.); h.wasisto@tu-braunschweig.de (H.S.W.)

Abstract

Gallium nitride (GaN) film delamination is an important process during the fabrication of GaN light-emitting diodes (LEDs) and laser diodes. Here, we utilize 520 nm femtosecond laser pulses, exploiting non-linear absorption rather than single-photon absorption like in conventional laser lift-off (LLO) utilizing excimer or Q-switched laser sources. The focus of this study is to investigate the influence of laser scanning speed and integrated fluence corresponding with laser energy per area during the LLO processing of GaN LED chips and their resulting structural properties. Since both sapphire substrate and InGaN/GaN heterostructures are fully transparent to the emission of the laser system, a key question is related to the impact of laser pulses on the quality of thin film structure. Therefore, several characterization methods (i.e., scanning electron microscopy (SEM), atomic force microscopy (AFM), X-ray diffraction (XRD), Raman spectroscopy, and electroluminescence

spectroscopy) were employed to understand the material modifications made by femtosecond LLO (*fs*-LLO). We demonstrated that by adjusting the laser scanning speed, smooth GaN surfaces and good crystal quality could be obtained regardless of the existing delamination of metal contact, which then slightly downgraded the LED performance. Here, the integrated fluence level was set in the range of 2.6 to 4.4 J/cm^2 to enable the *fs*-LLO process. Moreover, two mitigation strategies were developed and proven to improve the optoelectrical characteristics of the lifted-off LEDs (i.e., modification of processing step related to the metal creation and reduction of laser energy).

Keywords: laser lift-off, gallium nitride, LED, femtosecond laser, chip integration, laser micromachining.

1. Introduction

Since their invention by Akasaki, Amano, and Nakamura in the early 1990s, gallium nitride (GaN)-based blue light-emitting diodes (LEDs) have been continuously developed into a mature optoelectronic technology. Nowadays, these semiconductor structures are employed not only in conventional solid-state lighting, but also other applications (e.g., visible light communication,[1,2] gas sensors,[3,4] vertical nanowire arrays,[5,6] portable lensless microscopes,[7] and opto-microbial fuel cell diagnostics[8]). Furthermore, the focus of GaN LED research and development has been shifted from the basic material quality enhancement into advanced processing methods to support the creation of tailored optoelectronic devices. These include both monolithic and hybrid integrations of GaN LEDs with electronics or other functional devices.[8–10] Although the former can provide more highly integrated structures and smaller devices, the latter is now becoming more favorable. This is due to the fact that the monolithic fabrication of GaN LEDs driven by high-electron mobility transistors (HEMTs) requires very complex material growth process, in which normally the performance of one of those devices has to be compromised.[11] Meanwhile, for hybrid-integrated systems, both components can be optimized in separate processes resulting in the highest possible device performance.[1] Moreover, they can be realized on specific materials other than their original epitaxial substrates (e.g., conductive or flexible substrates).[11–13] In most cases, GaN LEDs are grown on sapphire (Al_2O_3) as substrates due to the lack of GaN homo-substrates. However, they exhibit poor electrical and thermal conductivities (~35 W/mK).[14] Even for GaN LEDs grown on Si or metal substrates with high electrical and thermal conductivities, the lattice mismatch and thermal expansion coefficients between GaN and its substrates lead to high dislocation and crack densities in the epitaxial layers.[15,16] Thus, the transfer of LED structures grown on sapphire onto a more suitable carrier (e.g. Cu foil with thermal conductivity of up to 300 W/mK) has become a way to go to yield optimum device performance.[17]

Laser lift-off (LLO) is a method that is proven to be fast and non-chemical for removing the thin GaN layer stack from the sapphire substrate and then transferring it onto a potential foreign carrier substrate. The first LLO-based GaN film detachment from sapphire substrate was demonstrated using a third-harmonic Q-switched Nd:YAG laser with 355 nm wavelength [18]. Laser pulses with this wavelength were transmitted through the sapphire substrate onto the GaN/sapphire interface and absorbed in the GaN interface region. The photon absorption

induced decomposition of GaN into metallic Ga and gaseous N_2. Conventionally, LLO can be performed using a variety of short-pulsed lasers, including the excimer lasers (e.g., 193-nm ArF, 248-nm KrF, and 308 nm XeCl lasers) and Q-switched lasers (e.g., with frequency-tripled (355 nm) or quadrupled (266 nm) nanosecond laser).[19] In the optoelectronic industry, KrF excimer lasers with 248 nm emission are often applied for the LLO procedure using raster scanning method.[20] This conventional LLO approach requires direct absorption in the semiconductor. Although that lift-off process has been mature and commonly used in the LED industry, nowadays several research groups have been attempting to find other methods that might offer more benefits in terms of the material processing flexibility (e.g., use of a single laser system for different LED material types like AlN buffer layer in UV LEDs, growth of sacrificial layers like graphene or other 2D materials between the active LED layer stack and its substrate, and utilization of mechanical peel-off and chemical solution for chip separation).[21–25]

Here, we explored a new alternative method, which uses ultrashort pulses of laser source with photon energies below the band gap of the semiconductor and the non-linear optical response in the high excitation regime. Under these circumstances, multi-photon absorption sets in for LLO purposes. Unlike the conventional LLO, in this study we employed a laser source emitting at 520 nm (2.38 eV) with the photon energy lower than the GaN bandgap (3.4 eV). Thus, linear absorption can be neglected. Furthermore, the extremely high laser intensities during the ultrashort pulse times enable a higher order process, which in this case is mainly two-photon absorption. Moreover, decreasing the laser pulse duration will further suppress the thermal effect caused by laser-material interaction (e.g., from 350 to 100 fs). Thus, laser-induced crystal damages can be minimized during ablation process.[26] Meanwhile, choosing a femtosecond laser source at the visible wavelength (e.g., 520 nm) offers straightforward optical alignment during sample preparation. Another laser source with a longer wavelength of 1030 nm (near infrared) but with the same pulse width of 350 fs could also be opted resulting in multiphoton absorption instead of only two-absorption. This technique has been reported to slice GaN thin film from its original bulk substrate (i.e., bulk GaN).[25]

In our previous study, the femtosecond LLO (*fs*-LLO) at a wavelength of 520 nm had been used to release free-standing bare GaN LED films with an area of 0.5 × 0.5 mm^2 from sapphire.[27] Although the laser beam characteristics and the laser-induced damage threshold for GaN (0.5 J/cm^2) had been determined, the GaN LED chips were not fully fabricated as a complete functional device in cleanroom yet (i.e., *n*-GaN etching was not performed and metal contacts (electrodes) were not realized). As a result, electroluminescence was not able to be conducted because of their chip fragility and incomplete structure. Moreover, the effects of laser scanning speed and integrated fluence during *fs*-LLO were not investigated in detail. Material characteristic assessments (e.g., Raman spectroscopy, X-ray diffraction (XRD) analysis, and atomic force microscopy (AFM)) had not been carried out. Thus, several questions still need to be answered, especially related to the feasibility of this method to transfer the functioning GaN LED devices from their original substrates to other substrates, without damaging the quantum well area and degrading the material and optical characteristics. In this paper, we attempt to demonstrate a fast physical transfer of InGaN/GaN LED chips from sapphire to flexible substrate (copper (Cu) foil) using *fs*-LLO, in which their crystal quality, surface morphology, and electroluminescence were investigated in detail. The GaN LEDs have

been created as fully functional devices, where metal contacts were also integrated on their surfaces. It is worth mentioning that besides laser energy and wavelength, the scanning type consisting of scanning speed, repetition, and step width has been a crucial parameter for the LLO process.[28] Thus, we examined this parameter influence in combination with the integrated laser fluence (Φ_{int}), which is the total laser energy per area. After demonstrating the delamination of GaN LED stack from the original sapphire substrate, we then transferred it onto a Cu foil. Finally, the quality of lifted-off GaN LED chips was characterized to detect their possible degradations after *fs*-LLO.

2. Materials and Methods

2.1 Materials

GaN LEDs with a peak wavelength of 470 nm were epitaxially grown on 430 µm thick two-inch c-plane (0001) double-side polished (DSP) transparent sapphire substrates by metalorganic vapour-phase epitaxy (MOVPE) inside an Aixtron G3 reactor in epitaxy competence center (ec²). The DSP sapphire was used to facilitate light transmission from the wafer backside during the *fs*-LLO process. The InGaN/GaN films with a total thickness of ~5 µm consisted of a 2.4 µm thick *n*-GaN buffer layer with a dopant concentration of 10^{18} cm^{-3}, a 2.1 µm heavily doped *n*-GaN layer with a dopant concentration of 10^{18} - 10^{19} cm^{-3}, 4 pairs of InGaN/GaN multi quantum wells (MQWs), and a *p*-GaN layer with a total thickness of ~300 nm. To activate the *p*-GaN layer, the LEDs were annealed in the MOVPE reactor at 770 °C for 20 min.[29]

2.2 Femtosecond laser lift-off

The experimental setup for performing the *fs*-LLO is sketched in **Figure 1a**. A laser source with a wavelength of 520 nm, a pulse width of 350 fs, and a repetition rate of 200 kHz was used. The incident laser from an Yb-based commercial fs laser source (SPIRIT-1040, Spectra-Physics) passed through a galvanometer scanner heading to a telecentric *f*-theta objective lens and sequentially being directed to a sample positioner underneath. The mirrors inside the galvanometer scanner allowed fast x-y beam scanning along the sample surface with a velocity of up to 2.5 m/s, where the incident angle was kept orthogonal onto the surface by the telecentric objective.

The *fs*-LLO method was conducted by scanning a laser beam across the backside of a sapphire substrate to separate and transfer the processed GaN LED chips onto a target substrate (e.g., metal foil). In the LLO process, the sapphire substrate must be DSP and transparent for accommodating the path of photons toward the GaN/Sapphire layer interface. For the conventional LLO, the energy of the photons must be higher than the bandgap of GaN (hv > 3.4 eV). Hence, the pulse energy can be directly absorbed at the GaN region near the GaN/sapphire interface (red bar in **Figure 1b-left**), which leads to the thermal decomposition of GaN into metallic Ga and gaseous N_2 at temperature of up to 900 °C.[30] Unlike the conventional LLO, the impinging photons from the ultrashort laser pulse possess lower energy (2.38 eV) than the GaN bandgap (3.4 eV). Nonetheless, the high photon density leads to two-photon absorption mechanism.[31] Laser pulses transmitted through the sapphire can reach to and subsequently be absorbed in the GaN region near the GaN/sapphire interface (red bar) by a

two-photon absorption process. The decomposition of GaN yielded at that interface causes a subsequent detachment of the GaN layer from the sapphire (**Figure 1b-right**).

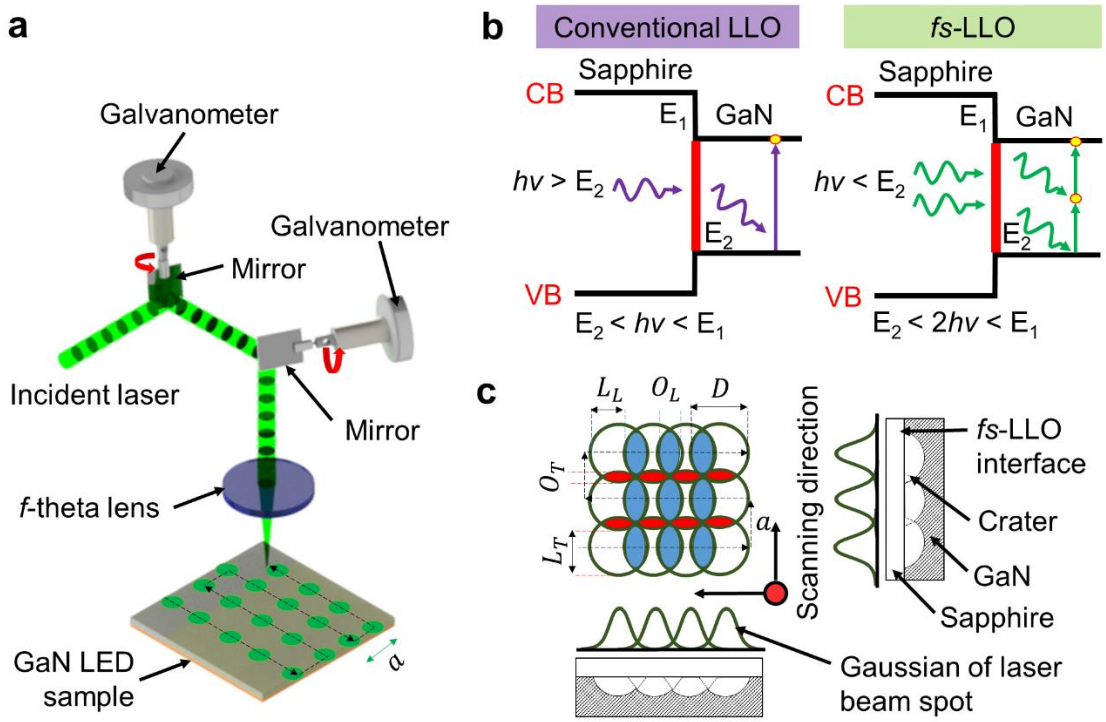

Figure 1 a Laser micromachining setup integrated with a telecentric *f*-theta objective lens and a Galvanometer scanner for *fs*-LLO from the backside of LED wafer. **b** Band diagrams for conventional LLO and *fs*-LLO processing of GaN on sapphire substrate illustrating single and two-photon absorption procedures, respectively. **c** Laser scanning scheme showing overlap, Gaussian energy distribution, and crater patterns for the proposed *fs*-LLO.

From our former investigation, the integrated fluence values of between 1 and 5 J/cm^2 were utilized to lift bare GaN LED films from their sapphire substrate.[27] Here, it is worth mentioning that the required integrated fluence in *fs*-LLO is significantly higher than that in conventional LLO (i.e., ranging from 0.1 to 1 J/cm^2).[30,32,33] In this study, the laser pulse energy (E_p) was kept constant at ~3.3 µJ per pulse corresponding to a peak fluence (Φ_0) of ~1.5 J/cm^2 at the sample plane per laser pulse. Here, laser focus position on target surface has a beam width (2ω) of ~20 µm. Employing this pulse energy level was proven to be able to yield a high lift-off success rate of up to ~70%.[27] Nonetheless, the scanning strategy has been modified from cross-line to parallel-line scanning pattern, because the former was ineffective resulting from the inhomogeneous impinging photons on the *fs*-LLO interface. Meanwhile, the latter could reduce the number of laser beam hitting the surface during *fs*-LLO (see **Figure 1a**). Therefore, considering the needed threshold integrated fluence, we have decided to use the integrated fluence ranging from ~2.5 to ~4.5 J/cm^2 to guarantee a successful lift-off process of the GaN LED films.[27]

Besides the laser energy, the distance between laser spots is a major factor for the overall *fs*-LLO scanning process, since it determines the degree of overlap between subsequent laser spots. The lateral overlap length or distance between two consecutive laser shots (L_L) in scan direction on the sample is related to the scanning speed (v) and the pulse frequency (f) by:

$$L_L = \frac{v}{f} \quad \ldots (1)$$

In transverse direction, the overlap length (L_T) can be controlled by the step width of the Galvanometer-scanner or track displacement. The applied scanning pattern, the Gaussian energy distribution of laser spots, and the craters generated by the beams on the sample surfaces are illustrated in **Figure 1c**. L_L and L_T are crucial values, since they determine the overlap of subsequent spots and therefore have a strong influence on the laser impact on the sample. Moreover, in laser micromachining process, the degree of overlap influences roughness and pattern homogeneity of the sample surface.[34,35] To describe the situation, we define the degree of overlap (%) by the following equations:[36]

$$O_L = \left(1 - \frac{L_L}{D}\right) \times 100\% \quad \ldots (2)$$

$$O_T = \left(1 - \frac{a}{D}\right) \times 100\% \quad \ldots (3)$$

where O_L and O_T are the percentage amounts of overlap between the diameters of two consecutive pulses in lateral and transverse directions, respectively. Meanwhile, D, a, f, and v represent diameter crater that is caused by the beam spot on GaN surface, track displacement (transverse pitch between passes), pulse frequency, and scanning speed of the laser beam, respectively. During the experiments, the first three parameters were kept at constant values of D = 20 µm, f = 200 kHz, and a = 10 µm, respectively, while v was varied from 1.5 m/s to 2.5 m/s with 0.5 m/s intervals.

Additionally, the integrated fluence (Φ_{int}) value is influenced by pulse energy (E_p) and the number of pulses per area (n/A). Therefore, according to Equation (1), the number of pulses per area and integrated fluence are calculated by:

$$n/A = \frac{1}{a} \times \frac{f}{v} \quad \ldots (4)$$

$$\Phi_{int} = E_p \times n/A \quad \ldots (5)$$

According to Equations (2) and (3), L_L and L_T can be increased by reducing the laser scanning speed (v) and the transverse pitch between two scans (a), respectively. Meanwhile, the n/A can be lowered by increasing the laser scanning speed. As a result, the value of integrated fluence can be lowered by increasing laser scanning speed (see Equations (4) and (5)).

2.3 Chip integration

The chip integration processing steps of the *fs*-LLO-based LEDs onto a flexible copper (Cu) foil (3M 1181 copper foil tape) are depicted in **Figures 2a-h**. First, a two-inch epitaxial GaN LED wafer was diced to a size of 1 cm × 1 cm and cleaned for 5 min in a 1 : 1 boiled

mixture of H_2O_2 (30% w.t.) and H_2SO_4 (98% w.t.), followed by a dip in 6.5% buffered hydrofluoric (HF) acid to detach any remaining organic impurity. To enhance the adhesion of photoresist onto the GaN surface during patterning, the sample was coated with hexamethyldisilazane (HMDS) (**Figure 2a**). Afterwards, multiple UV-photolithography processes were carried out employing a SUSS MJB4 mask aligner to fabricate the LED chips. After depositing and patterning a chemically inert and stable etching mask of ~300 nm chromium (Cr) onto the desired micro LED geometries using optical lithography, electron beam evaporation, and chemical lift-off process, the rest of the GaN material that was not protected by the mask was etched away using combined dry and wet etching processes.

Due to the highly energetic ion bombardment during the inductively coupled plasma reactive ion etching (ICP-RIE) in an SI 500C plasma dry etcher (Sentech Instruments GmbH, Germany), rough structures and numerous defects appeared on the GaN surface (see **Figure S1** in Supporting Information). Differentiating from the etching formula for silicon-based micro-/nanodevices that were normally performed at cryogenic temperature using SF_6/O_2 plasma and photoresist mask,[37–40] here, a typical dry etching recipe (i.e., ICP power of 800 W, HF power of 275 W, pressure of 0.5 Pa, SF_6/H_2 fluxes of 12 sccm and 100 sccm (standard cubic centimeter per minute), and room temperature) was used for 20 minutes with a Cr mask, which yielded an etch rate of ~1 µm/min. Afterwards, the sample was subsequently treated in a potassium hydroxide (KOH)-based wet chemical etchant to smoothen the GaN surface at a temperature of 80 °C for 20 minutes. From other reported studies using hydroxide ions (OH^-) as an active etchant, it was found that Ga- and N-polar GaN materials possess different etching behaviors.[41–43] As a key prerequisite for anisotropic KOH-etching to occur on GaN, the hydroxide ions have to be able to access the Ga atom for oxidation process. Thus, hexagonal pyramids can be formed when N-polar GaN areas were exposed to KOH solution.[41] However, Ga-polar regions could not be etched by KOH etchant and they would remain perfectly intact. Nonetheless, in case of many defects presented in the material (e.g., like the condition of the GaN surface after ICP-RIE in **Figure S1**), a higher number in dangling or defective Ga bonds generate local etch pit formation. This has led to an opportunity for hydroxide ions to reach Ga atoms in defect-rich areas progressing the wet etching process.[42,43] More detailed explanation and characteristics of this hybrid etching method combining both ICP-RIE and KOH-based wet etching processes on different stacks of GaN layers have been described in our former studies and the reports from other groups.[42–46] We have also demonstrated to employ this hybrid etching technique for realizing both field-effect transistors (FETs) and LEDs based on vertical GaN nanowire arrays.[1,5,47,48]

During metallization process, Pd/Au (2/10 nm), Pd/Au (20/150), and Cr/Au (50 /200 nm) were deposited using electron beam evaporation method, serving as the semi-transparent spreading layer, *p*-GaN, and *n*-GaN contacts, respectively (see **Figure 2b**). Using this semi-transparent stack metal composition, ~50% level of optical transmittance at a wavelength of 470 nm could be revealed. Furthermore, the sample was annealed at a temperature of 400 °C for 1 minute using rapid thermal annealing (RTA) to enhance the Ohmic contact property yielding a resistance of ~20 Ω.[4]

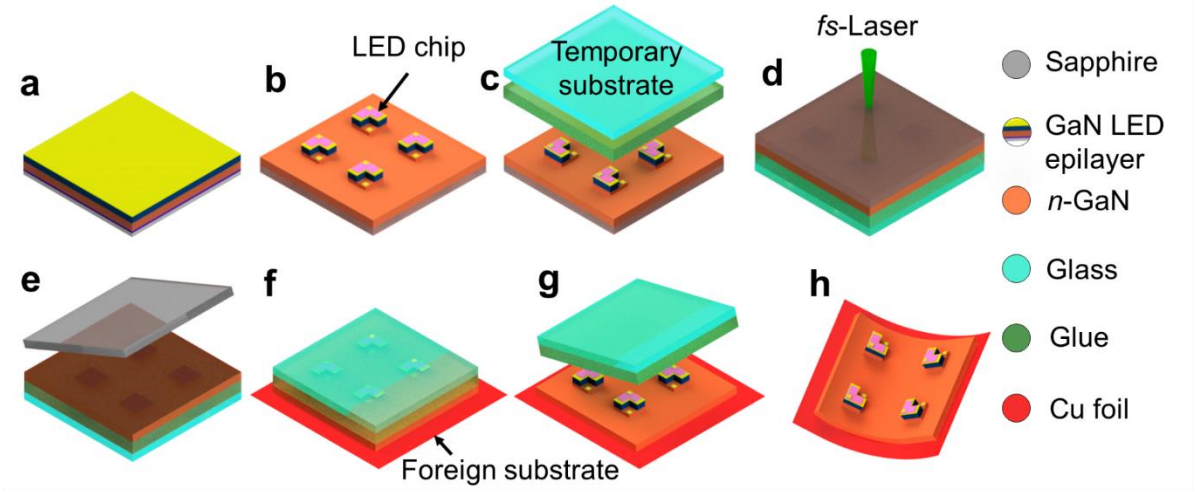

Figure 2 Schematics of the device processing steps to create GaN LEDs on a metal foil substrate using femtosecond laser lift-off (*fs*-LLO). **a** Wafer cleaning and preparation. **b** Top-down processing of GaN LEDs arranged as an array including photolithography, inductively coupled plasma reactive ion etching (ICP-RIE), wet etching, and metallization. **c** Bonding of GaN LED chips onto borosilicate glass as a temporary substrate. **d** Femtosecond LLO processing. **e** Removal of the sapphire substrate. **f** Transfer of GaN LED layer onto a metal foil. **g** Detachment of the glue and temporary substrate. **h** Fabricated GaN LEDs on a metal foil.

The transfer of the LED chips began with bonding of the sample onto a temporary substrate of borosilicate glass utilizing crystal bond glue (Plano GmbH, Germany) at a temperature of 120 °C to form a stacking structure of sapphire/GaN LED/adhesive/borosilicate glass (**Figure 2c**). Laser irradiation was then directed from the transparent sapphire substrate with a pulse energy of 3.3 µJ (**Figure 2d**). As a result, this *fs*-LLO process was able to detach the GaN layer containing LED chip array from the sapphire and subsequently to fasten it onto a borosilicate glass substrate (**Figure 2e**). After removing residual Ga that was produced during LLO on the sample using a mixture of HCl : H_2O (1 : 1) for 2 minute,[49] the LED chips were then transferred onto a Cu metal foil (**Figure 2f**). The adhesion between those two materials was made feasible at a temperature of 120°C, where the crystal glue simultaneously melted. The sample stack was then cleaned from the residue of adhesive glue with acetone (**Figure 2g**). Once the temporary substrate had been pulled away from the LED chips, they were able to be attached to the Cu foil (**Figure 2h**). As a final step, the integrated GaN LED devices were placed in a probe station equipped with microneedles and an optical fiber for further optoelectrical characterization.

2.4 Characterization

To characterize the crystalline qualities of the GaN LED before and after *fs*-LLO, a high-resolution XRD spectroscopy system with a Bruker D8 XRD Advance with Cu Kα radiation (λ = 0.154 nm) at acceleration voltage and current of 40 kV and 40 mA, respectively. The measurements were performed in a Bragg-Brentano (θ-2θ) configuration. Additionally, Raman spectra were measured using a Horiba HR800 spectrometer with a (500:1) polarized 20 mW

He-Ne laser having a wavelength of 632.8 nm. For observing the condition of GaN surface morphology and roughness, a scanning electron microscope (SEM, Leica Cambridge S360FE) and an atomic force microscope (AFM, Veeco Dimension 3100) in tapping mode were employed, respectively. The electroluminescence measurements of GaN LEDs were conducted using a semiconductor characterization system (4200-SCS Keithley, Keithley Instruments GmbH) and a spectrometer (USB HR 4000, Ocean Optics Inc.). The GaN LED chip cross-section after *fs*-LLO was investigated in a focused ion beam scanning electron microscope (FIB-SEM, Thermo Scientific Helios 5 UX DualBeam). All these characterizations were carried out at room temperature.

3. RESULTS AND DISCUSSION

Ultrashort-pulse laser micromachining with femtosecond laser as a light source can prevent thermal effects during the irradiation on a semiconductor.[26] Its principal absorption process during LLO using a pulse width of 350 fs and a wavelength of 520 nm differs from that in conventional LLO (nanosecond LLO). In particular, the ultrashort time of laser–material interaction can reduce the heating effects caused by the laser-induced shockwave. Here, in fact, the laser pulse width is shorter than the lifetime of photoexcited charge carrier (~800 ps).[50,51]

In the *fs*-LLO process, an appropriate integrated fluence range affected by laser scanning speed should be well defined for obtaining the optimum outcome of the GaN LED structures. Accordingly, since the scanning speed v can influence the integrated fluence as well as the degree of overlap between two spots (O_L and O_T), this parameter has been firstly varied to study its effect on GaN surface. **Figures 3a-c** show the SEM images of GaN backside surfaces (*n*-GaN buffer layer) after LLO at different laser scanning speeds of 1.5, 2, and 2.5 m/s (i.e., v_1, v_2 and v_3). The regularities in the peaks and valleys of the surface textures are clearly a signature of the variation in scanning speed. The surface roughness changes for lifted-off GaN films are confirmed by AFM images. For all those three samples, the scanning was performed over a 30 × 30 μm^2 area. The calculated root-mean-square (RMS) roughness (S_q) values have been lowered from 130.3 to 67.8 nm when the scanning speed was increased from v_1 = 1.5 m/s to v_3 = 2.5 m/s, respectively. These values are comparable with that of the GaN film surface released by single KrF (248 nm) excimer nanosecond laser pulse (i.e., RMS roughness of ~50 nm).[52] That structure was successfully bonded onto silicon at a bonding temperature of 400 °C. Another GaN layer processed by conventional LLO exhibited a similar RMS value of (32 ± 5) nm, which was observed from the 400 μm^2 large AFM image.[53] The flatness of the lifted-off GaN structures can however be improved by optimizing the lift-off condition. In our case, the scanning speeds of v_2 and v_3 are considerably acceptable to be the appropriate parameters because of their low RMS values.

It has been demonstrated that regardless of the same employed pulse energy, rough and coarse structures of the GaN layers could be yielded when they were processed with shorter laser irradiation time. Here, the energy accumulation at a certain position becomes higher at the lower scanning speed condition because it is affected by the next pulse during the scanning process in certain area. Moreover, the amount of ablation occurred progressively with a higher integrated fluence causing a coarse and deeper crater on the surface. Comparatively, faster laser

scanning has resulted in smoother surfaces. The lateral and transverse overlap distances between two spots of O_L and O_T were also influenced, respectively.

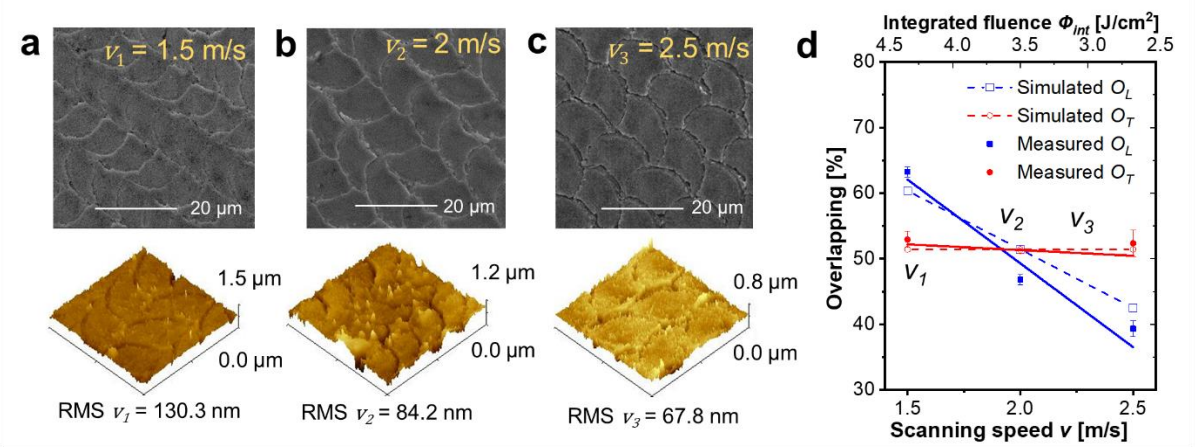

Figure 3 a-c SEM and AFM images of craters generated by femtosecond laser micromachining using different scanning speeds (v_1 – v_3) and **d** their corresponding measured and simulated beam overlapping rates ($\boldsymbol{O_L}$ and $\boldsymbol{O_T}$).

To analyze the resulting lifted-off structures, the theoretical crater spot diameter on GaN surface D of 20 µm from our previous report was used as a reference in a simulation involving Equations (2) and (3) to calculate both O_L and O_T values (**Figure 3d**). While O_L became smaller linearly as the laser scanning speed increased, O_T exhibited only a slight shift. From the experiments, the values of O_L shrank from 63.2 % to 39.3 % and those of O_T were relatively stable at ~50 %, when the laser scanning speed was changed from 1.5 to 2.5 m/s, respectively (see **Table S1**). Similar to the effect on the beam overlap, increasing the laser scanning speed could lower the number of pulse hitting on GaN surface per area. For instance, an increase in the number of pulses per area led to a higher integrated laser fluence, from 2.6 to 4.4 J/cm^2 as calculated using Equation (5). Therefore, an overlapping value of ~50% at v_2 for both O_L and O_T indicates the most equal level of the laser beam impinging on a certain area of the GaN surface during the laser scanning procedure. Under this condition, the resulting GaN film after *fs*-LLO will possess higher homogeneity, which is beneficial when the larger area needs to be realized.

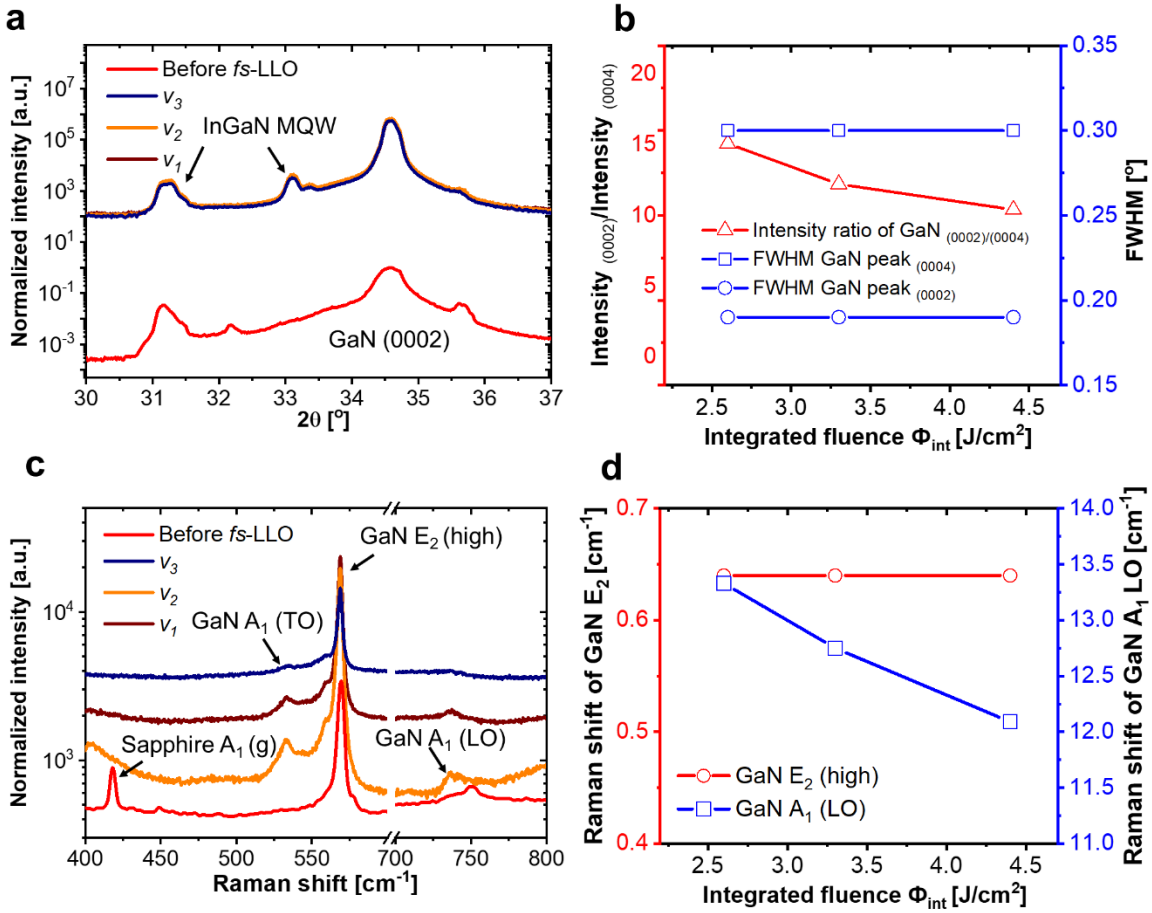

Figure 4 a X-ray diffractograms of the GaN LED structures before and after *fs*-LLO. **b** Intensity ratio of GaN LED after *fs*-LLO and FWHM value from XRD measurement. **c** Raman spectra of the GaN LED structures before and after *fs*-LLO. **d** Comparison of Raman shifts of GaN LED before and after *fs*-LLO.

From the X-ray diffractograms of InGaN/GaN LED shown in **Figure 4a**, hexagonal GaN (0002) and InGaN MQW peaks are exhibited in the diffraction patterns.[30,54–56] The measured full width at half maximum (FWHM) values of the GaN (0002) and GaN (0004) peak remained unchanged (i.e., 0.19° and 0.31°) for the three lifted-off GaN film samples treated with different integrated fluence levels as shown in **Figure 4b and S2**. On the other hand, intensity ratio between GaN (0002) and GaN (0004) changes due to increasing intensity of GaN (0004) on faster scanning speed condition. Thus, it indicates that the time of scanning process during femtosecond laser irradiation may affect the produced crater depth in GaN film but does not play a significant role to change the crystallite size. Nonetheless, for the conventional LLO, the phenomenon is different because the thermal effect is dominant during laser ablation process, which may affect the resulting crystal size.[28] Furthermore, the small peak of sapphire (00012) appearing in **Figure S2** indicates that sapphire debris was also involved during *fs*-LLO and transfer process for the lowest scanning speed.

By means of the Raman spectra shown in **Figure 4c**, the GaN layers possessed the E_2 mode peaks at 569.3 cm^{-1} and 568.8 cm^{-1} for the GaN samples before and after *fs*-LLO with different scanning speeds (v_1 - v_3), respectively. The A_1 longitudinal-optical (LO) phonon mode

peaks were found at 761.5 cm^{-1}, 737.4 cm^{-1}, 736.7 cm^{-1}, and 736.1 cm^{-1} for the samples before and after laser treatment with v_1-v_3, respectively. Based on the previously reported Raman spectroscopy studies on GaN[28,57] where the selection rules for the Raman peaks have been defined, only the E_2 (high) and A_1 (LO) modes were symmetry allowed in back scattering geometry with the laser beam incident on the (0001) surface. Thus, the GaN A_1 transverse-optical (TO) vibrational peak is prohibited. Nevertheless, in Figure 4c, the GaN A_1 (TO) peak is apparent at 533.5 cm^{-1} after *fs*-LLO, which may be due to the resulting rough GaN surface on the released *n*-GaN interface.[58] The GaN E_2 (high) phonon mode is normally used to quantify the stress value on GaN crystals. To further evaluate the samples, we then compared the GaN E_2 mode values of the samples before and after different laser treatments with that of unstressed GaN (i.e., 567.2 cm^{-1}).[59] The stress of the GaN layer (σ) can be calculated as $\sigma = \Delta\omega/k$, where k and $\Delta\omega$ are the Raman stress coefficient (-4.3 cm^{-1} GPa^{-1}) and the difference in the E_2 (high) phonon peaks between the stressed and unstressed GaN epilayers, respectively.

The compressive stress values for GaN LEDs before and after *fs*-LLO with different scanning speeds (v_1 - v_3) while being still attached on borosilicate glass were calculated to be 0.48 and 0.37 GPa, respectively. In fact, it is obvious that the GaN E_2 mode for all the three released samples possessed a constant Raman shift value of 0.64 cm^{-1} compared with that before *fs*-LLO (see **Figure 4d**). However, a different trend has been depicted in the GaN A_1 (LO) mode, in which its Raman shift value changed from 13.33 to 12.09 cm^{-1} when it was compared to that in original GaN A_1 (LO) before *fs*-LLO. In this case, the integrated fluence level was increased from 2.6 to 4.4 J/cm^2, respectively. Again, it should be noted that higher integrated fluence level corresponds to lower laser scanning speed during *fs*-LLO (see Equations (4) and (5)). The shifts of both E_2 and A_1 (LO) phonon mode peaks might be attributed to small stress effects, which changed the vibrational characteristics of the GaN thin films and led to the change of Raman frequency related to time of irradiation during *fs*-LLO scanning.[28]

After investigating and understanding the influences of integrated laser fluence on GaN material properties during *fs*-LLO, a complete GaN LED device on a foreign substrate (i.e., a Cu foil) was fabricated using the pre-determined *fs*-LLO parameters. Even though silicon or other conventional planar materials were normally employed as final substrate for such InGaN/GaN LED chips, we have selected Cu foil substrate because of its good electrical and high thermal conductivities as well as low price and high flexibility. A successful transfer on such an unconventional substrate like metal foil may open a path to realize inorganic flexible LED devices.[22] Here, the film surface roughness is a significant factor for the chip bonding. Having smooth film surface properties resulting from the *fs*-LLO can prevent the undesired gap or air bubble within the interface between the chip and the final substrate during bonding process.[52,60,61] Therefore, based on the experimental results of the laser impact on the GaN structures with constant pulse energy (E_p) at 3.3 μJ per pulse and varied scanning speeds (v_1 - v_3), the optimized GaN chip condition has been obtained at v_2 condition in terms of its surface morphology homogeneity and surface roughness level. Meanwhile, the crystal qualities of those three samples treated with different laser scanning speeds (v_1 - v_3) are almost identical. Here, we have demonstrated *fs*-LLO and transfer process of GaN LED chip from sapphire onto Cu foil using a parameter laser scanning speed v_2 = 2 m/s, which is equal to integrated laser

fluence (Φ_{int}) of 3.3 J/cm^2. The values of important parameters measured by different material characterization methods shown in **Figure 4** are listed in **Table S1**.

Figure 5(a) shows the XRD measurement results of the GaN LED before and after *fs*-LLO with pulse energy (E_p) of 3.3 μJ, in which laser scanning speed v_2 = 2 m/s (i.e., integrated laser fluence (Φ_{int}) of 3.3 J/cm^2) was used during laser processing. For the sample before *fs*-LLO (GaN LED on sapphire substrate), besides the two dominant GaN peaks (i.e., GaN (0002) and (0004)) that exhibited the orientations of hexagonal wurtzite GaN,[30,54,55] the X-ray diffractogram also shows an additional peak of sapphire (0006).[62] Meanwhile, after being lifted-off and transferred onto the Cu foil, that peak has been diminished and subsequently a new peak of Cu (200) existed instead.

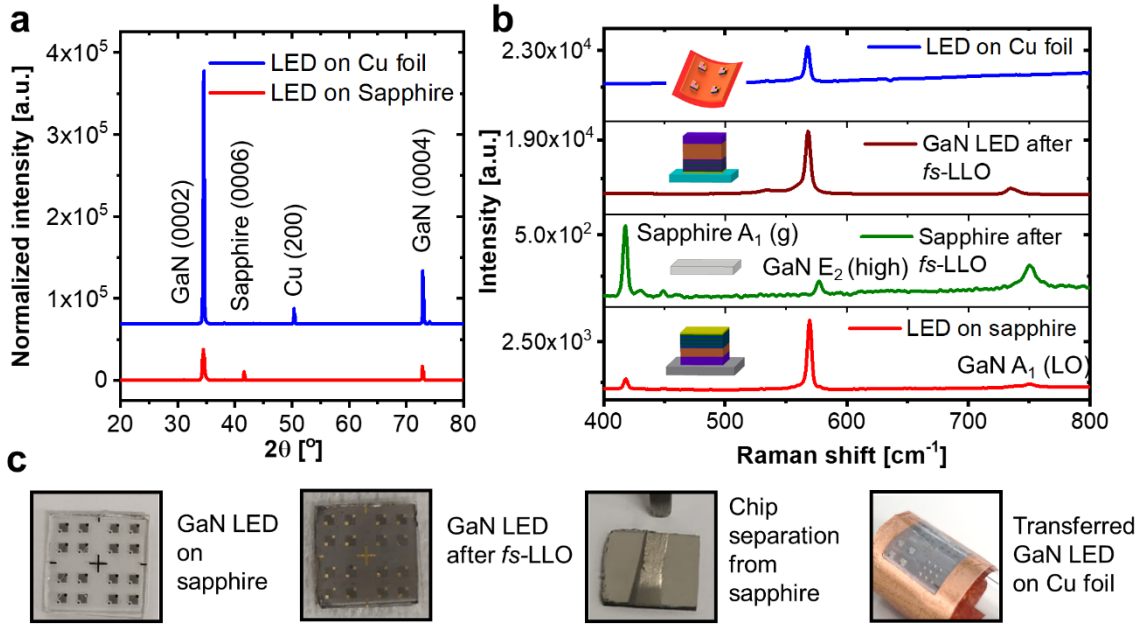

Figure 5. (a) XRD measurement results of the GaN LED structure before and after *fs*-LLO. (b) Raman spectra of the GaN LED on sapphire before *fs*-LLO, sapphire and GaN layer after *fs*-LLO, and GaN LED film after being transferred onto Cu foil substrate. (c) Photographs of fabricated GaN LED array on a Cu foil at different processing stages.

To further confirm a complete removal of sapphire in the transferred GaN LEDs, Raman spectra were measured for various sample conditions (i.e., GaN film on a sapphire substrate, the sapphire substrate after *fs*-LLO, GaN film on borosilicate glass after LLO, and GaN LED on flexible Cu foil substrate), as shown in **Figure 5b**. The GaN E_2 phonon mode peaks before and after *fs*-LLO (i.e., GaN on borosilicate glass) were located at 569.3 cm^{-1} and 568.8 cm^{-1}, respectively (see **Figure 5b**, red and brown curves).[11,57,59] However, after the LED chip has been transferred onto Cu foil, it shifted to lower wavenumber of 567.6 cm^{-1} (see **Figure 5b**, blue curve). This left Raman peak shifting indicates that during *fs*-LLO irradiation GaN LED layer thickness was decreased due to laser ablation that scraped away the GaN surface.[63] Being compared with the intrinsic E_2 (high) value of 567.2 cm^{-1} for stress-free GaN,[64,65] a residual compressive stress of 0.09 GPa was found in the GaN LED on Cu foil. This condition

points out that the GaN film has been relaxed from its previous states on sapphire before *fs*-LLO. In other words, GaN film on the new substrate has lower compressive stress than its as-grown condition.[11,57,59,66] Moreover, differentiating from the GaN side where no sapphire was found after *fs*-LLO, several GaN residues remained sticking on the sapphire side, which were designated by the existing GaN E_2 phonon mode at 577.1 cm^{-1} in the Raman scattering from the lifted sapphire surface due to laser irradiation process (see **Figure 5b**, green curve). **Table S2** lists the main material properties of GaN LEDs before and after *fs*-LLO measured by XRD and Raman spectroscopy, as displayed in **Figures 5a and b**. The conditions of GaN LED chips during the *fs*-LLO-based transfer process are depicted in **Figure 5c**. It is obvious that the separated LED chips could be integrated as an array in a defined area.

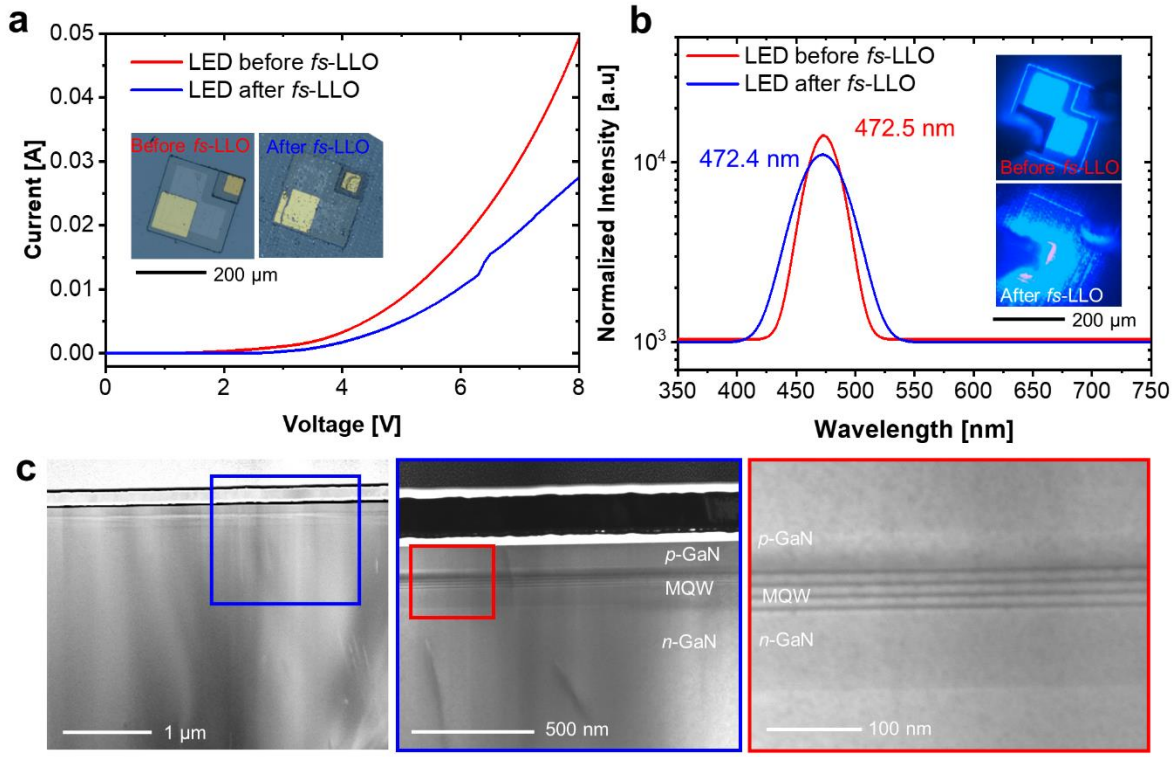

Figure 6 a I-V characteristics of GaN LED chips before and after *fs*-LLO. The inset shows the different conditions of the metal contacts on both chips. After *fs*-LLO, a few metal parts were peeled-off due to laser absorption. **b** Electroluminescent light spectra of the GaN LEDs before and after *fs*-LLO. The inset depicts that blue light emission of the transferred GaN LED was scattered due to the detachment of spreading thin film during *fs*-LLO process. **c** Cross-sectional profile of InGaN/GaN LED after *fs*-LLO processing investigated using a focused ion beam scanning electron microscope (FIB-SEM). The magnified picture shown crystal damage within *n*-GaN layer and complete condition of active area (InGaN/GaN MQWs).

To prove the LED device functionality after *fs*-LLO, an electroluminescence test was conducted. The current–voltage (I-V) characteristics and light emission spectra of the fabricated GaN LED chip on sapphire and the already-*fs* LLO-processed GaN LED chip on Cu foil measured at room temperature are shown in **Figures 6a and b**. The LED prior to *fs*-LLO exhibits a typical *p*–*n* diode behavior with a turn-on voltage of ~4 V at an injection current of 1 mA. The peak wavelength of the spectrum is found at 472.5 nm. Nonetheless, after *fs*-LLO

with an integrated laser fluence level of 3.3 J/cm^2, a slight performance degradation on the I-V curve was found from the GaN LED chip. Although the electroluminescence peak wavelength of the transferred LED chip was still at the similar position of 472.4 nm, its required turn-on voltage has become larger (~5 V). This phenomenon can easily be understood from the physical appearance of the LED chips in the insets of **Figure 6a**. Because of the excessively used laser energy and prolonged scanning time during the *fs*-LLO experiment, surface modification occurred on the metal contacts (i.e., several parts on the spreading layer and metal contact were peeled off). Regardless of the required optoelectrical performance optimization of the realized devices, this study has demonstrated a feasibility of using ultrashort pulse laser (femtosecond laser) to completely transfer InGaN/GaN LED chips from their original sapphire substrate onto a Cu foil. For the next study, the pulse energy (E_p) can be considered as another key factor to maintain the quality of GaN LED during *fs*-LLO besides scanning speed that has been discussed in this report (see **Figures S3c-e**).

The cross-sectional profile of a GaN LED on Cu foil that has been processed in *fs*-LLO using integrated fluence of $\Phi_{int} = 3.3$ J/cm^2 was investigated in an FIB-SEM, as depicted in in **Figures 6c**. Here, the photon energy that was expected to be only absorbed at GaN/sapphire interface has revealed a deeper penetration beyond that area. Although the InGaN/GaN MQW layers were still in a good condition (i.e., no significant defect was shown), a damage still appeared within the *n*-GaN layer, which is at around ~2 μm from the *fs*-LLO-released interface. This result is similar to those obtained in other previously reported LLO cases,[33,67,68] in which the location of structural defects or damages depends on the used laser pulse width and its absorption coefficient of GaN. One of the studies related to structural damages occurring in LLO processes has demonstrated that a laser possessing a higher absorption coefficient of GaN will yield shallower penetration depth (e.g., a 248 nm KrF excimer laser with a pulse time of 35 ns).[33] Thus, its photon energy would be mostly absorbed around the GaN/sapphire interface, where such a long pulse time results in a shock wave causing a dense dislocation and deforming the superficial structure. However, for lasers having lower absorption coefficient (e.g., a 355 nm Nd:YAG laser with a pulse time of 5 ns or a 520 nm Yb laser with a pulse width of 350 fs like in our case), a deeper penetration could occur causing more dislocations in the bulk region. In other words, lasers with a shorter laser pulse width tends to provide deeper impact or longer defect path inside the LED structure that may even reach to its MQW or *p*-GaN layer. Moreover, our experimental results suggest that during the fabrication of LED in a cleanroom, the metallization for both *p*- and *n*-contacts should be moved to the final device processing step and performed after the *fs*-LLO transfer procedure to avoid any possible laser-induced damage or surface modification on the metal contacts. This solution has been proven in **Figure S4**, where the lifted-off GaN LED chip with the metallization performed after *fs*-LLO exhibits a good I-V characteristic with a typical threshold voltage of ~3 V. The metal contacts are also crackless (i.e., no damage on the metal surface). It should be however noted that semitransparent metal spreading layer was not used in this case. Hence, the emitted light was only concentrated near to the edge of *p*-GaN contact.

Furthermore, in comparison to its conventional counterpart, the *fs*-LLO may offer several potential advantages. Considering its basic working principle of multi-photon absorption, the solid-state femtosecond laser and its optical setup can act conceivably as a versatile system to

transfer other semiconductor materials with higher band gap (e.g., AlN and AlGaN) that are often utilized as buffer layer for UV LEDs from their original to target substrates. This will not be possible when a conventional LLO process based on direct photon absorption is used, because then each laser type with certain pulse width is only able to be used for lifting a specific material having band gap less than its emitted photon energy. In addition to the InGaN LEDs, we had implemented the *fs*-LLO technique to separate the AlGaN UV LEDs from their sapphire substrates with different integrated fluences, i.e., 2.6 – 4.4 J/cm^2 (see **Figure S5** in Supporting Information). Regardless of the severe issues on the metal contacts that were peeled off during *fs*-LLO, the results suggest that the proposed transfer method offers a high processing flexibility for the target LED materials based on GaN.

Besides, the lower thermal effect occurring during ablation in *fs*-LLO may also potentially reduce the heating issue when the to-be-lifted-off LED chips have been firstly bonded with other active electronic devices that are sensitive to high temperature change. However, all these potential benefits still need to be proven, in which further investigations are necessary to fully comprehend the thermal influences as well as the other physical phenomena in *fs*-LLO process, including the ones from theory or simulation. Before conducting further experiment on the more complex material system (e.g., AlGaN UV LED), clear understanding and strong proof-of-concept using InGaN blue LED have to be obtained, as this technology has been commonly used as baseline in many optoelectronic applications. Hence, a comparison of its results with those obtained by conventional LLO that were already reported in literature can then directly be made.

4. CONCLUSIONS

We have processed InGaN/GaN-based LEDs on a sapphire substrate and transferred them with a 520 nm femtosecond laser via a two-step transfer method onto a foreign substrate (Cu foil). Prior to full LED device fabrication, one of the key femtosecond laser lift-off (*fs*-LLO) parameters (i.e., laser scanning speed that is related to integrated fluence level) has been investigated in detail, revealing that modifications of roughness, thickness, and crystalline quality might occur on the lifted-off thin GaN films when different scanning speeds were used during laser irradiation. The lateral and transverse overlap distances between two spots (O_L and O_T) were suggested to be set at ~50 % with an integrated fluence of 3.3 J/cm^2 to produce homogeneous GaN surface. Besides the scanning electron micrographs, the Raman and XRD spectra have been measured to comprehend the feasible changes in device material properties. From the optoelectrical characterization by means of electroluminescence test, it has been shown that a few damages of the metal contacts occurred resulting in a slightly higher required turn-on voltage (i.e., a voltage shift of ~1 V). However, the light emission peak wavelength was able to be kept at the similar position (~472 nm). The sequence of the LED fabrication steps in the cleanroom has been modified by defining the metallization as the final step after the *fs*-LLO transfer process to completely solve the metal contact issue. We finally note that the viability of our multi-photon non-linear LLO using femtosecond laser on GaN technology would require further quantitative insights on the quality (e.g., quantum efficiency) of the InGaN/GaN multi quantum wells (MQWs). Additionally, despite the already conducted FIB-

SEM investigation, photoluminescence spectroscopy and transmission electron microscopy (TEM) studies are needed to shed light on the MQW quality.

5. ASSOCIATED CONTENT

5.1 Supporting Information

Hybrid etching of GaN LED; Summarized material parameters; XRD spectra of GaN LEDs after fs-LLO; Defects on GaN LED metal contacts; GaN LED with modified metallization processing step; AlGaN UV LED on Cu foil after fs-LLO.

5.2 Author Contributions

N.Y. and H.S.W. conceived the idea, designed the experiment, formulated the materials, interpreted the experimental data, wrote the initial manuscript, and revised the paper. N.Y. fabricated the LEDs in cleanroom, creating figures in the paper, and performed femtosecond laser lift-off (fs-LLO) processing. N.Y. and S.B. prepared for the laser machining setup and optimized the parameters. G.T.M.K., S.G., and F.F.A. conducted Raman spectroscopy and XRD measurements. H.S.W. and K.T. provided inputs on material characteristic analysis. N.M. performed AFM measurements. H.S.W. and A.W. led, supervised, and coordinated the project. All authors discussed the results and approved the final manuscript.

5.3 Notes

The authors declare no competing interest.

ACKNOWLEDGEMENTS

This work was funded in part by the Lower Saxony Ministry for Science and Culture (N-MWK) within the group of “LENA-OptoSense”, in part by the European Union’s Horizon 2020 research and innovation program within the project of “ChipScope – Overcoming the Limits of Diffraction with Super- Resolution Lighting on a Chip” under grant agreement no 737089, and in part by the Deutsche Forschungsgemeinschaft (DFG, German Research Foundation) within “Excellence Strategy of EXC-2123 QuantumFrontiers – 390837967”. The authors thank Christoph Margenfeld and Irene Manglano Clavero for GaN wafer preparation in the epitaxy competence center (ec2). Nursidik Yulianto acknowledges the Ministry of Research, Technology and Higher Education of the Republic of Indonesia (RISTEKDIKTI) for the Ph.D. scholarship of RISET-Pro under no. 345/RISET-Pro/FGS/VIII/2016 and the Indonesian-German Centre for Nano and Quantum Technologies (IG-Nano) for the support. The authors thank Angelika Schmidt, Juliane Breitfelder, and Aileen Michalski for their technical support during the experiments, as well as Prof. Winfried Daum for providing AFM tool.

References

(1) Wasisto, H. S.; Prades, J. D.; Gülink, J.; Waag, A. Beyond Solid-State Lighting: Miniaturization, Hybrid Integration, and Applications of GaN Nano-and Micro-LEDs. *Appl. Phys. Rev.* **2019**, *6* (4). https://doi.org/10.1063/1.5096322.

(2) Chen, S. W. H.; Huang, Y. M.; Chang, Y. H.; Lin, Y.; Liou, F. J.; Hsu, Y. C.; Song, J.; Choi, J.; Chow, C. W.; Lin, C. C.; Horng, R. H.; Chen, Z.; Han, J.; Wu, T; Kuo, H. C. High-Bandwidth Green Semipolar (20-21) InGaN/GaN Micro Light-Emitting Diodes for Visible Light Communication. *ACS Photonics* **2020**, *7* (8), 2228–2235. https://doi.org/10.1021/acsphotonics.0c00764.

(3) Casals, O.; Markiewicz, N.; Fabrega, C.; Gràcia, I.; Cane, C.; Wasisto, H. S.; Waag, A.; Prades, J. D. A Parts per Billion (Ppb) Sensor for NO 2 with Microwatt (MW) Power Requirements Based on Micro Light Plates. *ACS Sensors* **2019**, *4* (4), 822–826. https://doi.org/10.1021/acssensors.9b00150.

(4) Markiewicz, N.; Casals, O.; Fabrega, C.; Gràcia, I.; Cané, C.; Suryo, H.; Waag, A.; Prades, J. D.; Gr, I. Micro Light Plates for Low-Power Photoactivated (Gas) Sensors Micro Light Plates for Low-Power Photoactivated (Gas) Sensors. **2019**, *053508* (October 2018). https://doi.org/10.1063/1.5078497.

(5) Mariana, S.; Gülink, J.; Hamdana, G.; Yu, F.; Strempel, K.; Spende, H.; Yulianto, N.; Granz, T.; Prades, J. D.; Peiner, E.; Wasisto, H. S.; Waag, A. Vertical GaN Nanowires and Nanoscale Light-Emitting-Diode Arrays for Lighting and Sensing Applications. *ACS Appl. Nano Mater.* **2019**, *2* (7), 4133–4142. https://doi.org/10.1021/acsanm.9b00587.

(6) Wang, X.; Li, S.; Mohajerani, M. S.; Ledig, J.; Wehmann, H. H.; Mandl, M.; Strassburg, M.; Steegmüller, U.; Jahn, U.; Lähnemann, J.; Riechert, J.; Griffiths, I.; Cherns, D.; Waag, A. Continuous-Flow MOVPE of Ga-Polar GaN Column Arrays and Core-Shell LED Structures. *Cryst. Growth Des.* **2013**, *13* (8), 3475–3480. https://doi.org/10.1021/cg4003737.

(7) Scholz, G.; Mariana, S.; Dharmawan, A. B.; Syamsu, I.; Hörmann, P.; Reuse, C.; Hartmann, J.; Hiller, K.; Prades, J. D.; Wasisto, H. S.; Waag, A. Continuous Live-Cell Culture Imaging and Single-Cell Tracking by Computational Lensfree LED Microscopy. *Sensors (Switzerland)* **2019**, *19* (5), 1–13. https://doi.org/10.3390/s19051234.

(8) Schmidt, I.; Gad, A.; Scholz, G.; Boht, H.; Martens, M.; Schilling, M.; Suryo Wasisto, H.; Waag, A.; Schröder, U. Gold-Modified Indium Tin Oxide as a Transparent Window in Optoelectronic Diagnostics of Electrochemically Active Biofilms. *Biosens. Bioelectron.* **2017**, *94*, 74–80. https://doi.org/10.1016/j.bios.2017.02.042.

(9) Liu, Z. J.; Huang, T.; Ma, J.; Liu, C.; Lau, K. M. Monolithic Integration of AlGaN/GaN HEMT on LED by MOCVD. *IEEE Electron Device Lett.* **2014**, *35* (3), 330–332. https://doi.org/10.1109/LED.2014.2300897.

(10) Guan, N.; Dai, X.; Messanvi, A.; Zhang, H.; Yan, J.; Gautier, E.; Bougerol, C.; Julien, F. H.; Durand, C.; Eymery, J.; Tchernycheva, M. Flexible White Light Emitting Diodes Based on Nitride Nanowires and Nanophosphors. *ACS Photonics* **2016**, *3* (4), 597–603. https://doi.org/10.1021/acsphotonics.5b00696.

(11) Seo, J. H.; Li, J.; Lee, J.; Gong, S.; Lin, J.; Jiang, H.; Ma, Z. A Simplified Method of Making Flexible Blue LEDs on a Plastic Substrate. *IEEE Photonics J.* **2015**, *7* (2). https://doi.org/10.1109/JPHOT.2015.2412459.

(12) Kuo, H.; Wang, S.; Wang, P.; Uang, K.; Chen, T.; Chen, S.; Lee, W. Use of Elastic Conductive Adhesive as the Bonding Agent for the Fabrication of Vertical Structure GaN-Based LEDs on Flexible Metal Substrate. **2008**, *20* (7), 523–525.

(13) Dai, X.; Messanvi, A.; Zhang, H.; Durand, C.; Eymery, J.; Bougerol, C.; Julien, F. H.; Tchernycheva, M. Flexible Light-Emitting Diodes Based on Vertical Nitride Nanowires. *Nano Lett.* **2015**, *15* (10), 6958–6964. https://doi.org/10.1021/acs.nanolett.5b02900.
(14) Horng, R. H.; Chiang, C. C.; Hsiao, H. Y.; Zheng, X.; Wuu, D. S.; Lin, H. I. Improved Thermal Management of GaN/Sapphire Light-Emitting Diodes Embedded in Reflective Heat Spreaders. *Appl. Phys. Lett.* **2008**, *93* (11), 2006–2009. https://doi.org/10.1063/1.2983740.
(15) Bessolov, V. N.; Konenkova, E. V.; Orlova, T. A.; Rodin, S. N.; Seredova, N. V.; Solomnikova, A. V.; Shcheglov, M. P.; Kibalov, D. S.; Smirnov, V. K. Properties of Semipolar GaN Grown on a Si(100) Substrate. *Semiconductors* **2019**, *53* (7), 989–992. https://doi.org/10.1134/S1063782619070054.
(16) May, B. J.; Sarwar, A. T. M. G.; Myers, R. C. Nanowire LEDs Grown Directly on Flexible Metal Foil. *Appl. Phys. Lett.* **2016**, *108* (14). https://doi.org/10.1063/1.4945419.
(17) Tian, X.; Chen, W.; Zhang, J. Thermal Design for the High-Power LED Lamp. *J. Semicond.* **2011**, *32* (1), 1–4. https://doi.org/10.1088/1674-4926/32/1/014009.
(18) Kelly, M. K.; Ambacher, O.; Dahlheimer, B.; Groos, G.; Dimitrov, R.; Angerer, H.; Stutzmann, M. Optical Patterning of GaN Films. *Appl. Phys. Lett.* **1996**, *69* (12), 1749–1751. https://doi.org/10.1063/1.117473.
(19) Kim, J.; Kim, J. H.; Cho, S. H.; Whang, K. H. Selective Lift-off of GaN Light-Emitting Diode from a Sapphire Substrate Using 266-Nm Diode-Pumped Solid-State Laser Irradiation. *Appl. Phys. A Mater. Sci. Process.* **2016**, *122* (4), 1–6. https://doi.org/10.1007/s00339-016-9928-7.
(20) Delmdahl, R.; Pätzel, R.; Brune, J.; Senczuk, R.; Goßler, C.; Moser, R.; Kunzer, M.; Schwarz, U. T. Line Beam Processing for Laser Lift-off of GaN from Sapphire. *Phys. Status Solidi Appl. Mater. Sci.* **2012**, *209* (12), 2653–2658. https://doi.org/10.1002/pssa.201228430.
(21) Aoshima, H.; Takeda, K.; Takehara, K.; Ito, S.; Mori, M.; Iwaya, M.; Takeuchi, T.; Kamiyama, S.; Akasaki, I.; Amano, H. Laser Lift-off of AlN/Sapphire for UV Light-Emitting Diodes. *Phys. Status Solidi Curr. Top. Solid State Phys.* **2012**, *9* (3–4), 753–756. https://doi.org/10.1002/pssc.201100491.
(22) Yang, G.; Jung, Y.; Cuervo, C. V.; Ren, F.; Pearton, S. J.; Kim, J. GaN-Based Light-Emitting Diodes on Graphene-Coated Flexible Substrates. *Opt. Express* **2014**, *22* (S3), A812. https://doi.org/10.1364/oe.22.00a812.
(23) Ayari, T.; Sundaram, S.; Li, X.; El Gmili, Y.; Voss, P. L.; Salvestrini, J. P.; Ougazzaden, A. Wafer-Scale Controlled Exfoliation of Metal Organic Vapor Phase Epitaxy Grown InGaN/GaN Multi Quantum Well Structures Using Low-Tack Two-Dimensional Layered h-BN. *Appl. Phys. Lett.* **2016**, *108* (17). https://doi.org/10.1063/1.4948260.
(24) Lin, M. S.; Lin, C. F.; Huang, W. C.; Wang, G. M.; Shieh, B. C.; Dai, J. J.; Chang, S. Y.; Wuu, D. S.; Liu, P. L.; Horng, R. H. Chemical-Mechanical Lift-off Process for InGaN Epitaxial Layers. *Appl. Phys. Express* **2011**, *4* (6). https://doi.org/10.1143/APEX.4.062101.
(25) Voronenkov, V.; Bochkareva, N.; Gorbunov, R.; Zubrilov, A.; Kogotkov, V.; Latyshev, P.; Lelikov, Y.; Leonidov, A.; Shreter, Y. Laser Slicing: A Thin Film Lift-off Method for GaN-on-GaN Technology. *Results Phys.* **2019**, *13* (March), 27–30. https://doi.org/10.1016/j.rinp.2019.102233.
(26) Rethfeld, B.; Ivanov, D. S.; Garcia, M. E.; Anisimov, S. I. Modelling Ultrafast Laser Ablation. *J. Phys. D. Appl. Phys.* **2017**, *50* (19). https://doi.org/10.1088/1361-6463/50/19/193001.
(27) Bornemann, S.; Yulianto, N.; Spende, H.; Herbani, Y.; Prades, J. D.; Wasisto, H. S.; Waag, A. Femtosecond Laser Lift-Off with Sub-Bandgap Excitation for Production of

Free-Standing GaN Light-Emitting Diode Chips. *Adv. Eng. Mater.* **2019**, *1901192*. https://doi.org/10.1002/adem.201901192.

(28) Tong, X. L.; Li, L.; Zhang, D. S.; Dai, Y. T.; Lv, D. J.; Ling, K.; Liu, Z. X.; Lu, P. X.; Yang, G.; Yang, Z. Y.; Long, H. The Influences of Laser Scanning Speed on the Structural and Optical Properties of Thin GaN Films Separated from Sapphire Substrates by Excimer Laser Lift-Off. *J. Phys. D. Appl. Phys.* **2009**, *42* (4). https://doi.org/10.1088/0022-3727/42/4/045414.

(29) Hartmann, J.; Steib, F.; Zhou, H.; Ledig, J.; Nicolai, L.; Fündling, S.; Schimpke, T.; Avramescu, A.; Varghese, T.; Trampert, A.; Straßburg, M.; Lugauer, H.J.; Wehmann, H.H.; Waag, A. Study of 3D-Growth Conditions for Selective Area MOVPE of High Aspect Ratio GaN Fins with Non-Polar Vertical Sidewalls. *J. Cryst. Growth* **2017**, *476*, 90–98. https://doi.org/10.1016/j.jcrysgro.2017.08.021.

(30) Ueda, T.; Ishida, M.; Yuri, M. Separation of Thin GaN from Sapphire by Laser Lift-off Technique. *Jpn. J. Appl. Phys.* **2011**, *50*. https://doi.org/10.1143/JJAP.50.041001.

(31) Vivas, M. G.; Manoel, D. S.; Dipold, J.; Martins, R. J.; Fonseca, R. D.; Manglano-Clavero, I.; Margenfeld, C.; Waag, A.; Voss, T.; Mendonca, C. R. Femtosecond-Laser Induced Two-Photon Absorption of GaN and AlxGa1-XN Thin Films: Tuning the Nonlinear Optical Response by Alloying and Doping. *J. Alloys Compd.* **2020**, *825*, 153828. https://doi.org/10.1016/j.jallcom.2020.153828.

(32) Wong, W. S.; Sands, T.; Cheung, N. W.; Kneissl, M.; Bour, D. P.; Mei, P.; Romano, L. T.; Johnson, N. M. Fabrication of Thin-Film InGaN Light-Emitting Diode Membranes by Laser Lift-Off. *Appl. Phys. Lett.* **1999**, *75* (10), 1360–1362. https://doi.org/10.1063/1.124693.

(33) Cheng, J.-H.; Wu, Y. S.; Peng, W. C.; Ouyang, H. Effects of Laser Sources on Damage Mechanisms and Reverse-Bias Leakages of Laser Lift-Off GaN-Based LEDs. *J. Electrochem. Soc.* **2009**, *156* (8), H640. https://doi.org/10.1149/1.3148251.

(34) Lehr, J.; Kietzig, A. M. Production of Homogenous Micro-Structures by Femtosecond Laser Micro-Machining. *Opt. Lasers Eng.* **2014**, *57*, 121–129. https://doi.org/10.1016/j.optlaseng.2014.01.012.

(35) Kibria, G.; Chatterjee, S.; Shivakoti, I.; Doloi, B.; Bhattacharyya, B. RSM Based Experimental Investigation and Analysis into Laser Surface Texturing on Titanium Using Pulsed Nd:YAG Laser. *IOP Conf. Ser. Mater. Sci. Eng.* **2018**, *377* (1). https://doi.org/10.1088/1757-899X/377/1/012203.

(36) Teixidor, D.; Grzenda, M.; Bustillo, A.; Ciurana, J. Modeling Pulsed Laser Micromachining of Micro Geometries Using Machine-Learning Techniques. *J. Intell. Manuf.* **2015**, *26* (4), 801–814. https://doi.org/10.1007/s10845-013-0835-x.

(37) Wasisto, H. S.; Merzsch, S.; Waag, A.; Uhde, E.; Salthammer, T.; Peiner, E. Airborne Engineered Nanoparticle Mass Sensor Based on a Silicon Resonant Cantilever. *Sensors Actuators, B Chem.* **2013**. https://doi.org/10.1016/j.snb.2012.04.003.

(38) Wasisto, H. S.; Merzsch, S.; Stranz, A.; Waag, A.; Uhde, E.; Salthammer, T.; Peiner, E. Silicon Resonant Nanopillar Sensors for Airborne Titanium Dioxide Engineered Nanoparticle Mass Detection. *Sensors Actuators, B Chem.* **2013**. https://doi.org/10.1016/j.snb.2013.02.053.

(39) Wasisto, H. S.; Merzsch, S.; Uhde, E.; Waag, A.; Peiner, E. Handheld Personal Airborne Nanoparticle Detector Based on Microelectromechanical Silicon Resonant Cantilever. *Microelectron. Eng.* **2015**. https://doi.org/10.1016/j.mee.2015.03.037.

(40) Wasisto, H. S.; Merzsch, S.; Stranz, A.; Waag, A.; Uhde, E.; Salthammer, T.; Peiner, E. Silicon Nanowire Resonators: Aerosol Nanoparticle Mass Sensing in the Workplace. *IEEE Nanotechnol. Mag.* **2013**. https://doi.org/10.1109/MNANO.2013.2260462.

(41) Ng, H. M.; Weimann, N. G.; Chowdhury, A. GaN Nanotip Pyramids Formed by

Anisotropic Etching. *J. Appl. Phys.* **2003**, *94* (1), 650–653. https://doi.org/10.1063/1.1582233.

(42) Tautz, M.; Díaz Díaz, D. Wet-Chemical Etching of GaN: Underlying Mechanism of a Key Step in Blue and White LED Production. *ChemistrySelect* **2018**, *3* (5), 1480–1494. https://doi.org/10.1002/slct.201702267.

(43) Tautz, M.; Weimar, A.; Graßl, C.; Welzel, M.; Díaz Díaz, D. Anisotropy and Mechanistic Elucidation of Wet-Chemical Gallium Nitride Etching at the Atomic Level. *Phys. Status Solidi Appl. Mater. Sci.* **2020**, *2000221* (September). https://doi.org/10.1002/pssa.202000221.

(44) Fatahilah, M. F.; Strempel, K.; Yu, F.; Vodapally, S.; Waag, A.; Wasisto, H. S. 3D GaN Nanoarchitecture for Field-Effect Transistors. *Micro Nano Eng.* **2019**, *3* (December 2018), 59–81. https://doi.org/10.1016/j.mne.2019.04.001.

(45) Yu, F.; Yao, S.; Römer, F.; Witzigmann, B.; Schimpke, T.; Strassburg, M.; Bakin, A.; Schumacher, H. W.; Peiner, E.; Wasisto, H. S.; Waag, A. GaN Nanowire Arrays with Nonpolar Sidewalls for Vertically Integrated Field-Effect Transistors. *Nanotechnology* **2017**, *28* (9). https://doi.org/10.1088/1361-6528/aa57b6.

(46) Park, J.; Song, K. M.; Jeon, S. R.; Baek, J. H.; Ryu, S. W. Doping Selective Lateral Electrochemical Etching of GaN for Chemical Lift-Off. *Appl. Phys. Lett.* **2009**, *94* (22), 1–4. https://doi.org/10.1063/1.3153116.

(47) Debnath, R.; Ha, J.-Y.; Wen, B.; Paramanik, D.; Motayed, A.; King, M. R.; Davydov, A. V. Top-down Fabrication of Large-Area GaN Micro- and Nanopillars. *J. Vac. Sci. Technol. B, Nanotechnol. Microelectron. Mater. Process. Meas. Phenom.* **2014**, *32* (2), 021204. https://doi.org/10.1116/1.4865908.

(48) Ruzzarin, M.; Meneghini, M.; De Santi, C.; Neviani, A.; Yu, F.; Strempel, K.; Fatahilah, M. F.; Witzigmann, B.; Wasisto, H. S.; Waag, A.; Meneghesso, G.; Zanoni, E. Demonstration of UV-Induced Threshold Voltage Instabilities in Vertical GaN Nanowire Array-Based Transistors. *IEEE Trans. Electron Devices* **2019**, *66* (5), 2119–2124. https://doi.org/10.1109/TED.2019.2904851.

(49) King, S. W.; Barnak, J. P.; Bremser, M. D.; Tracy, K. M.; Ronning, C.; Davis, R. F.; Nemanich, R. J. Cleaning of AlN and GaN Surfaces. *J. Appl. Phys.* **1998**, *84* (9), 5248–5260. https://doi.org/10.1063/1.368814.

(50) Grinys, T.; Dmukauskas, M.; Ščiuka, M.; Nargelas, S.; Melninkaitis, A. Evolution of Femtosecond Laser-Induced Damage in Doped GaN Thin Films. *Appl. Phys. A Mater. Sci. Process.* **2014**, *114* (2), 381–385. https://doi.org/10.1007/s00339-013-8103-7.

(51) Ozono, K.; Obara, M.; Usui, A.; Sunakawa, H. High-Speed Ablation Etching of GaN Semiconductor Using Femtosecond Laser. *Opt. Commun.* **2001**, *189* (1–3), 103–106. https://doi.org/10.1016/S0030-4018(01)01002-1.

(52) Zhang, X.; Ruan, Y.; Chen, S.; Li, C. GaN/Metal/Si Heterostructure Fabricated by Metal Bonding and Laser Lift-Off. *J. Semicond.* **2009**, *30* (12), 10–14. https://doi.org/10.1088/1674-4926/30/12/123001.

(53) Kim, H. S.; Dawson, M. D.; Yeom, G. Y. Surface Properties of GaN Fabricated by Laser Lift-off and ICP Etching. *J. Korean Phys. Soc.* **2002**, *40* (4), 567–571. https://doi.org/https://doi.org/10.3938/jkps.40.567.

(54) Liu, Y.; Qin, F.; Zhang, D.; Bian, J.; Zhao, Y.; Wang, E.; Wang, S.; Zhong, M.; Ju, Z. Low-Temperature Growth of Highly c-Oriented GaN Films on Cu Coated Glass Substrates with ECR-PEMOCVD. *J. Cryst. Growth* **2013**, *368*, 92–96. https://doi.org/10.1016/j.jcrysgro.2013.01.033.

(55) Harutyunyan, V. S.; Aivazyan, A. P.; Weber, E. R.; Kim, Y.; Park, Y. High-Resolution x-Ray Diffraction Strain – Stress Analysis of GaN / Sapphire Heterostructures. *J. Phys. D. Appl. Phys.* **2001**, *34*, A35–A39.

(56) Horng, R.; Shen, K.; Kuo, Y.; Wuu, D. The Performance of GaN LEDs Using an Embedded Finger-Type Contact GaN Light Emitting Diodes with Wing-Type Imbedded Contacts. **2014**, No. June 2018. https://doi.org/10.1117/12.2037274.

(57) Kuball, M. Raman Spectroscopy of GaN, AlGaN and AlN for Process and Growth Monitoring/Control. *Surf. Interface Anal.* **2001**, *31* (10), 987–999. https://doi.org/10.1002/sia.1134.

(58) Chen, W. H.; Hu, X. D.; Shan, X. D.; Kang, X. N.; Zhou, X. R.; Zhang, X. M.; Yu, T. J.; Yang, Z. J.; You, L. P.; Xu, K.; Zhang, G.Y. Shock-Assisted Superficial Hexagonal-to-Cubic Phase Transition in GaN/Sapphire Interface Induced by Using Ultra-Violet Laser Lift-of Techniques. *Chinese Phys. Lett.* **2009**, *26* (1). https://doi.org/10.1088/0256-307X/26/1/016203.

(59) Park, B. G.; Saravana Kumar, R.; Moon, M. L.; Kim, M. D.; Kang, T. W.; Yang, W. C.; Kim, S. G. Comparison of Stress States in GaN Films Grown on Different Substrates: Langasite, Sapphire and Silicon. *J. Cryst. Growth* **2015**. https://doi.org/10.1016/j.jcrysgro.2015.03.009.

(60) Mu, F.; Morino, Y.; Jerchel, K.; Fujino, M.; Suga, T. GaN-Si Direct Wafer Bonding at Room Temperature for Thin GaN Device Transfer after Epitaxial Lift Off. *Appl. Surf. Sci.* **2017**, *416*, 1007–1012. https://doi.org/10.1016/j.apsusc.2017.04.247.

(61) Wang, T.; Liu, B.; À, X. G.; Fang, Y.; Shen, G. Integration of GaN Thin f Ilms with Silicon Substrates by Fusion Bonding and Laser Lift-Off. *Chinese Opt. Lett.* **2006**, *4* (7), 416–418.

(62) Kushvaha, S. S.; Kumar, M. S.; Maurya, K. K.; Dalai, M. K.; Sharma, N. D. Highly C-Axis Oriented Growth of GaN Film on Sapphire (0001) by Laser Molecular Beam Epitaxy Using HVPE Grown GaN Bulk Target. *AIP Adv.* **2013**. https://doi.org/10.1063/1.4821276.

(63) Hushur, A.; Manghnani, M. H.; Narayan, J. Raman Studies of GaN/Sapphire Thin Film Heterostructures. *J. Appl. Phys.* **2009**, *106* (5). https://doi.org/10.1063/1.3213370.

(64) Horng, R.-H.; Tien, C.-H.; Chuang, S.-H.; Liu, K.-C.; Wuu, D.-S. External Stress Effects on the Optical and Electrical Properties of Flexible InGaN-Based Green Light-Emitting Diodes. *Opt. Express* **2015**, *23* (24), 31334. https://doi.org/10.1364/oe.23.031334.

(65) Lin, P. J.; Tien, C. H.; Wang, T. Y.; Chen, C. L.; Ou, S. L.; Chung, B. C.; Wuu, D. S. On the Role of AlN Insertion Layer in Stress Control of GaN on 150-Mm Si (111) Substrate. *Crystals* **2017**, *7* (5). https://doi.org/10.3390/cryst7050134.

(66) Kisielowski, C.; Krüger, J.; Ruvimov, S.; Suski, T.; Ager, J.; Jones, E.; Liliental-Weber, Z.; Rubin, M.; Weber, E.; Bremser, M.; Davis, R.F. Strain-Related Phenomena in GaN Thin Films. *Phys. Rev. B - Condens. Matter Mater. Phys.* **1996**, *54* (24), 17745–17753. https://doi.org/10.1103/PhysRevB.54.17745.

(67) Bornemann, S.; Yulianto, N.; Gülink, J.; Margenfeld, C.; Meyer, T.; Wasisto, H. S.; Waag, A. Structural Modifications in Free-Standing InGaN/GaN LEDs after Femtosecond Laser Lift-Off. *Proceedings* **2018**, *2* (13), 897. https://doi.org/10.3390/proceedings2130897.

(68) Yulianto, N.; Bornemann, S.; Daul, L.; Margenfeld, C.; Manglano Clavero, I.; Majid, N.; Koenders, L.; Daum, W.; Waag, A.; Suryo Wasisto, H. Transferable Substrateless GaN LED Chips Produced by Femtosecond Laser Lift-Off for Flexible Sensor Applications †. **2018**, 3–6. https://doi.org/10.3390/proceedings2130891.

TOR Graphic

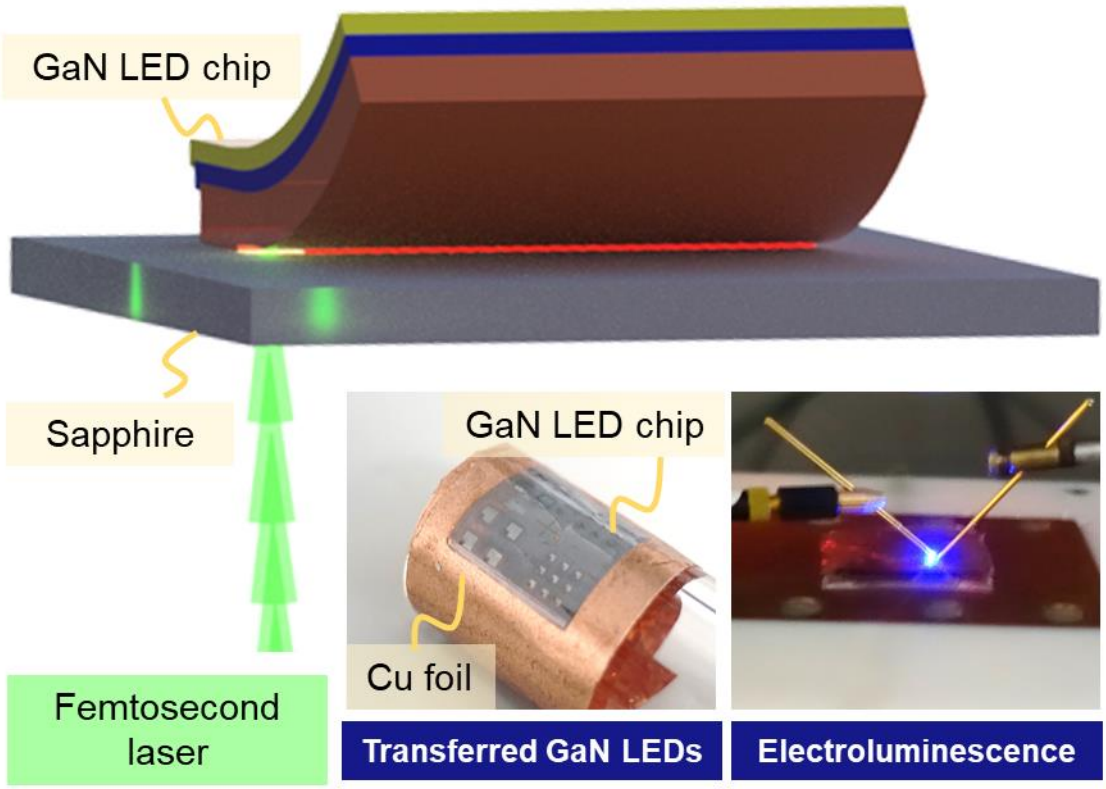
GaN LED chip
Sapphire
Femtosecond laser
GaN LED chip
Cu foil
Transferred GaN LEDs
Electroluminescence